OPEN ACCESS Freely available online

PLOS ONE

Potential Cooperations between Odorant-Binding Proteins of the Scarab Beetle *Holotrichia oblita* Faldermann (Coleoptera: Scarabaeidae)

Bing Wang, Li Guan, Tao Zhong, Kebin Li, Jiao Yin*, Yazhong Cao*

State Key Laboratory for Biology of Plant Diseases and Insect Pests, Institute of Plant Protection, Chinese Academy of Agricultural Sciences, Beijing, People's Republic of China

Abstract

It was previously thought that the odorant binding proteins (OBPs) in the sensillum lymph might serve as carriers, which could carry lipophilic odorant molecules to olfactory receptors. In this study, two novel OBP genes of the scarab beetle *Holotrichia oblita* were screened using an antennal cDNA library. The full cDNA of HoblOBP3 and HoblOBP4 was cloned using reverse transcription PCR and rapid amplification of the cDNA ends. Homology modeling of both OBPs was performed using SWISS-MODEL on-line tools. Next, the two OBPs were expressed in *Escherichia coli* and purified using Ni ion affinity chromatography. The ligand-binding properties of HoblOBP3 and HoblOBP4 in 42 ligands respectively were measured using the fluorescence probe N-phenyl-naphthylamine (1-NPN). The results obtained from competitive binding assays demonstrated that HoblOBP4 showed a broader range of binding affinities to the test compounds, while HoblOBP3 displays more specific binding affinity. Furthermore, other OBPs and CSPs were expressed in *Escherichia coli* and purified using Ni ion affinity chromatography. Binding curves were measured for binary mixtures of OBPs and CSPs using 1-NPN, and the Scatchard plots exhibited "J"-like nonlinear correlation trends in some samples. In addition, competitive binding assays of the HoblOBP1 and HoblOBP2 mixtures and of the HoblOBP2 and HoblOBP4 mixtures with representative compounds unexpectedly demonstrated good affinity, which revealed extreme differences that were only obtained using the individual proteins. In the immunocytochemical analysis, colocalization of HoblOBP1 and HoblOBP2, and of HoblOBP2 and HoblOBP4, was detected in the sensilla basiconica and sensilla placodea, respectively. All of these results suggested that HoblOBP1 and HoblOBP2, as well as HoblOBP2 and HoblOBP4, may serve as heterodimers in the sensillum lymph.

Citation: Wang B, Guan L, Zhong T, Li K, Yin J, et al. (2013) Potential Cooperations between Odorant-Binding Proteins of the Scarab Beetle *Holotrichia oblita* Faldermann (Coleoptera: Scarabaeidae). PLoS ONE 8(12): e84795. doi:10.1371/journal.pone.0084795

Editor: Narayanaswamy Srinivasan, Indian Institute of Science, India

Received April 11, 2013; **Accepted** November 19, 2013; **Published** December 23, 2013

Funding: The work was supported by the Special Fund for Agro-Scientific Research in the Public Interest (No. 201003025); and the Natural Science Foundation of China (No. 31000853). The funders had no role in study design, data collection and analysis, decision to publish, or preparation of the manuscript.

Competing interests: The authors have declared that no competing interests exist.

* E-mail: yzcao@ippcaas.cn (YC); jyin@ippcaas.cn (JY)

Introduction

The sophisticated insect olfactory system can detect and discriminate between different amounts of odorants, which are volatile small organic molecules in the environment. This characteristic property plays a crucial role in insect behaviors, such as host seeking, mating, ovipositing, as well as escape behaviors [1-5]. Indeed, the process of olfactory recognition involves several types of proteins, including odorant binding proteins (OBPs), olfactory receptors (ORs), odorant-degrading enzymes (ODEs), sensory neuron membrane proteins (SNMPs), and ionotropic receptors (IRs) [6]. OBPs exist at a high concentration (up to 10 mM) in the lymph of the antennal sensilla, which surrounds the dendrites of sensory neurons and functions as a carrier for lipophilic odorant molecules [5,7,8]. OBPs are commonly small molecule, water-soluble polypeptides, and exhibit six conserved cysteines that paired with three disulfide bridges in an interlocking fashion [6,9-14]. The first identified insect OBP was found in the giant moth *Antheraea polyphemus* [15]. Thus far, OBPs from more than 40 insect species belonging to eight different orders have been isolated and cloned [7]. However, these OBPs appear to be very divergent from those of other insect orders and are expressed in sensory organs, particularly in the antennae [16,17]. More recently, chemosensory proteins (CSPs), which are members of a second family of soluble polypeptides in insects, have been identified in the lymphs of various chemoreception organs [18-23], as well as in non-chemoreception organs [24-27]. In contrast to OBPs, CSPs are better conserved and more widely distributed in insect species

(10 orders) [7,12,22]. Within the last two decades, both classes of soluble proteins have been studied to understand their functions in insect chemoreception [12-14,22].

Although the molecular mechanism of these proteins as filters in the recognition of target odors is not yet completely understood, an olfactory model has been proposed. Two decades worth of reported studies have shown that various lipophilic odorants from the external surroundings can be captured and transported by OBPs into the sensillar lymph to activate ORs to initiate signal transduction [3,4,7]. Until recently, the involvement of OBPs in the recognition of olfactory stimuli has not been completely elucidated [6,7]. There are two exclusive functional patterns of OBPs. The first pattern suggests that ORs can be activated by the odorant itself (which has been observed in moths and in mosquitoes) [7,8]. If this assumption is true, then OBPs might exhibit binding and releasing functions [28-30]. A classical study performed on *Bombyx. mori* PBP showed that conformational changes enabled pheromones to enter the binding pocket in a neutral environment. However, as the pH changes from neutral to acidic, OBP-odorant complexes become unstable, and the pheromone molecule is released from the binding cavity [31,32]. Several similar studies have been performed in other insect orders, such as the OBPs of the cockroach *Leucophaea maderae* [33], giant moth *A. polyphemus*[34], *Amyelois. transitella* [35,36], *Anopholes gambiae* [37], *Aedes. aegypti* [38] and *Culex pipiens quinquefasciatus* [39]. Another pattern has indicated that ORs may be activated by an OBP-odorant complex, and that OBPs might be required for the interaction with ORs in insects [40], about which several experimental evidence has been provided [29,41]. LUSH, an OBP76a in *Drosophila Melanogaster*, is expressed in the sensillum lymph. T1 trichoid sensilla in wild-type flies respond to the aggregation pheromone vaccenyl acetate (VA). However, they cannot detect VA in the absence of the LUSH gene. Further studies have shown that the neuronal sensitivity to VA in the mutant flies may be rescued if LUSH is added in T1 sensilla [42]. This study provides evidence for the requirement of OBPs in olfactory recognition. Although related studies on the two patterns have been reported, this olfactory receptive mechanism is still not well understood.

A presumed function of the OBP has been previously proposed and indicates that OBPs can form dimers to carry ligands in union [37,43,44]. Although scattered evidence for OBP dimer formation in some insect species has been reported, there is still insufficient evidence for this hypothesis [45-49]. In an early study of OBPs in *A. gambiae*, a three-dimensional structure study has revealed that OBPs are present as dimers, and that their ligand-binding pockets connect from one end of the protein to the other, resulting in a continuous, long hydrophobic tunnel that may potentially allow passage of a ligand [37]. Indeed, this hypothesis is only an extrapolation based on an analysis of the crystal structure and the exceptionally high concentration of OBPs in the sensillar lymph. Additionally, another study on specific interactions among odorant-binding proteins in *A. gambiae* has demonstrated that OBPs are capable of forming homodimers and heterodimers [43]. This result may provide evidence to support the theory of a long hydrophobic tunnel mechanism. Furthermore, one recent study demonstrated unexpected binding characteristics of OBP mixtures (OBP1 and OBP4) in *A. gambiae* using fluorescence binding assays, which revealed OBP heterodimer formation [44]. Moreover, a co-expression study performed in the antennal sensilla of *A. gambiae* was consistent with previous studies. Although evidence of dimer formation in OBPs has been found in *A. gambiae*, whether this interacting mechanism exists *in vivo* or in other species requires further exploration.

Underground pests are a harmful class group in agriculture, and their ability to conceal themselves, and extensive feeding habits result in difficulties in the prevention and control of pests [50-52]. The scarab beetle, *Holotrichia oblita* Faldermann (Coleoptera: Scarabaeidae), belongs to such a class and has caused serious economic damage to crops, fruit trees and forest trees in China [13]. An environmentally friendly method for the control of *H. oblita* is needed. A better understanding of the olfactory processes may help to improve current insect control strategies, particularly those strategies that rely on deviation from their normal behaviors, such as pheromone-based traps [3,4,53,54]. Thus, studies on OBPs in *H. oblita* have quickly developed, and the ability to sequence the genome of the red flour beetle *Tribolium castaneum* has dramatically accelerated these studies [13,52,55]. Some evidence has indicated that OBPs in *H. oblita* and *Holotrichia parallela* are directly involved in the selective perception of volatilizing odors from the host plant and putative sex pheromones [13,52]. In addition, these results demonstrate that OBPs can distinguish between odorants according to their chain length, functional group and alkene geometry [56].

In the present study, we identified two OBPs from the antennae cDNA library of *H. oblita*, HoblOBP3 and HoblOBP4. We expressed both of these OBPs in a heterologous system and measured their ligand-binding activities using a fluorescence competitive binding assay with the N-phenyl-1-naphthyl-amine (1-NPN) fluorescent probe. In addition, other known HoblOBPs and HoblCSPs have been expressed using the same method. Binding curves with binary mixture groups indicated that HoblOBP2 interacted with either HoblOBP4 or HoblOBP1. We detected the co-expression of HoblOBP2 and HoblOBP4 and of HoblOBP2 and HoblOBP1 in the antennal sensilla of *H. Oblita* using double immunolabelling procedures and immunoelectron microscopy. Taken together, our results provide new evidence for olfactory recognition in underground pests.

Results

1 Sequences and homology analysis

Two partial sequences were obtained from the cDNA library of the *H. oblita* antennae screening. Full-length cDNAs encoding HoblOBP3 and HoblOBP4 were cloned from *H. oblita* and called HoblOBP3 and HoblOBP4 (GenBank IDs: ADX96030 and ADX96031). The ORF of the HoblOBP3 cDNA consisted of 429 nucleotides and encoded 143 amino acids. The predicted signal peptide contained the initial 21 amino acids, as identified using SignalP 4.1 software. The ORF was

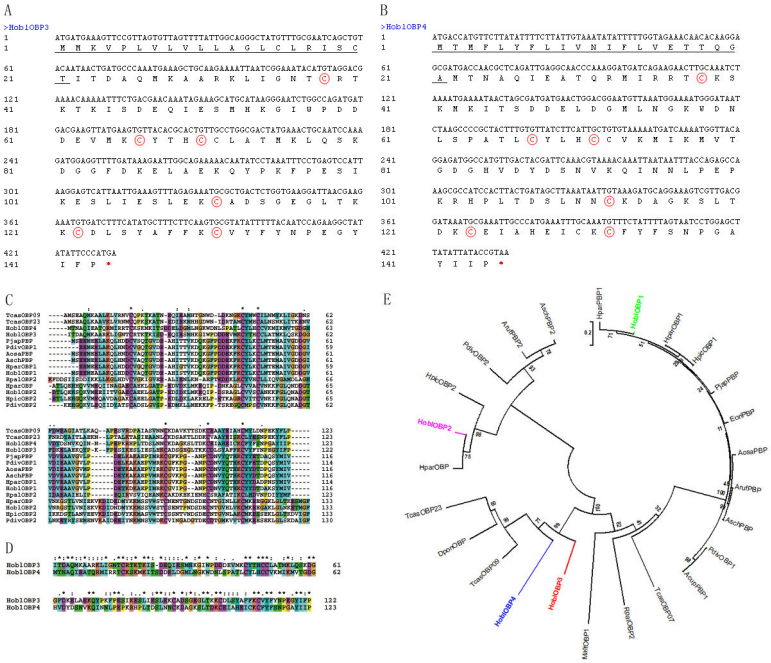

Figure 1. Characterization and phylogenetic analysis of HoblOBP3 and HoblOBP4. (**A**-**B**) The ORF of nucleotide sequence and deduced amino acid sequence of the OBP3 (**A**) and OBP4 (**B**) from H. *oblita*. The six conserved cysteines are indicated in rings with red color. The predicted signal peptide is underlined. The asterisk with red color marks the translation-termination codon. (**C**) Alignment of some OBPs amino acid sequence from Coleoptera insects. (**D**) Alignment of amino acid sequence between HoblOBP3 and HoblOBP4. (**E**) Phylogenetic tree of OBPs amino acid sequences in Coleoptera, including HoblOBPs. The corresponding OBPs in alignment and phylogenetic tree are listed as follow. RpalOBP2 (AAD31875, *Rhynchophorus palmarum*), DponOBP (AFI45058, *Dendroctonus ponderosae*), TcasOBP09 (EFA10713, *Tribolium castaneum*), TcasOBP23 (EFA10803, *Tribolium castaneum*), TcasOBP07 (EFA04593, *Tribolium castaneum*), HparOBP (AEA76516, *Holotrichia parallela*), HparPBP1 (ADF87391, *Holotrichia parallela*), HparOBP1 (BAC07272, *Holotrichia parallela*), HpicOBP1(BAC07270, *Heptophylla picea*), HpicOBP2 (BAC07271, *Heptophylla picea*), PjapPBP (AAC63436, *Popillia japonica*), EoriPBP (BAB70711, *Exomala orientalis*), AosaPBP (AAC63437, *Anomala osakana*), PdivOBP1 (BAA88061, *Phyllopertha diversa*), PdivOBP2(BAA88062, *Phyllopertha diversa*), AcupPBP1 (BAC06496, *Anomala cuprea*), ArufPBP (BAF79995, *Anomala rufocuprea*), ArufPBP2 (BAF91329, *Anomala rufocuprea*), AschPBP(BAF79599, *Anomala schonfeldti*), AschPBP2 (BAF79600, *Anomala schonfeldti*), MaltOBP1 (ABR53888, *Monochamus alternatus*), HoblOBP1(ACX32050, *Holotrichia oblita*), HoblOBP2(ACX32049, *Holotrichia oblita*), HoblOBP3 (ADX96030, *Holotrichia oblita*), HoblOBP4 (ADX96031, *Holotrichia oblita*).

doi: 10.1371/journal.pone.0084795.g001

terminated by a TGA stop codon. The predicted molecular weight and isoelectric point of the mature HoblOBP3 were 16.2 kDa and 6.71, respectively (Figure 1A). The ORF of the HoblOBP4 cDNA consisted of 432 nucleotides and encoded 144 amino acids. The predicted signal peptide contained the initial 21 amino acids. The ORF was terminated by a TAA stop codon. The predicted molecular weight and isoelectric point of the mature HoblOBP4 were 16.3 kDa and 6.87, respectively (Figure 1B). HoblOBP3 and HoblOBP4 contained a typical framework of OBPs (six conserved cysteines paired in three disulfide bridges), which belonged to the classical group of OBPs (Figure 1C-D). The conserved patterns are listed as follows: HoblOBP3: X16-Cys-X27-Cys-X3-Cys-X40-Cys-X10-Cys-X8-Cys-X12, HoblOBP4: X16-Cys-X28-Cys-X3-Cys-X40-Cys-X10-Cys-X8-Cys-X12, of which X represents any amino acid. The frameworks of HoblOBP3 and HoblOBP4 shared a high identity and were consistent with a “signature” for insect OBPs [7].

The sequence alignment between HoblOBP3 and HoblOBP4 was performed. These result showed that the amino acid identity received a low score and only reached 38% identity (Figure 1D). Multiple sequence alignment among the HoblOBPs and corresponding OBPs from other species of Coleoptera are shown in Figure 1C. HoblOBP3 and HoblOBP4 shared low identity (

< 41%) with other Coleoptera OBPs. The highest identities of HoblOBP3 and HoblOBP4 were 41% and 38% with TcasOBP09 (*T. castaneum*) and 41% and 34% with TcasOBP23 (*T. castaneum*), respectively (Figure 1C). These phylogenetic relationships indicated that HoblOBP3 and HoblOBP4 belonged to different branches than HoblOBP1 and HoblOBP2, which were consistent with their sequence

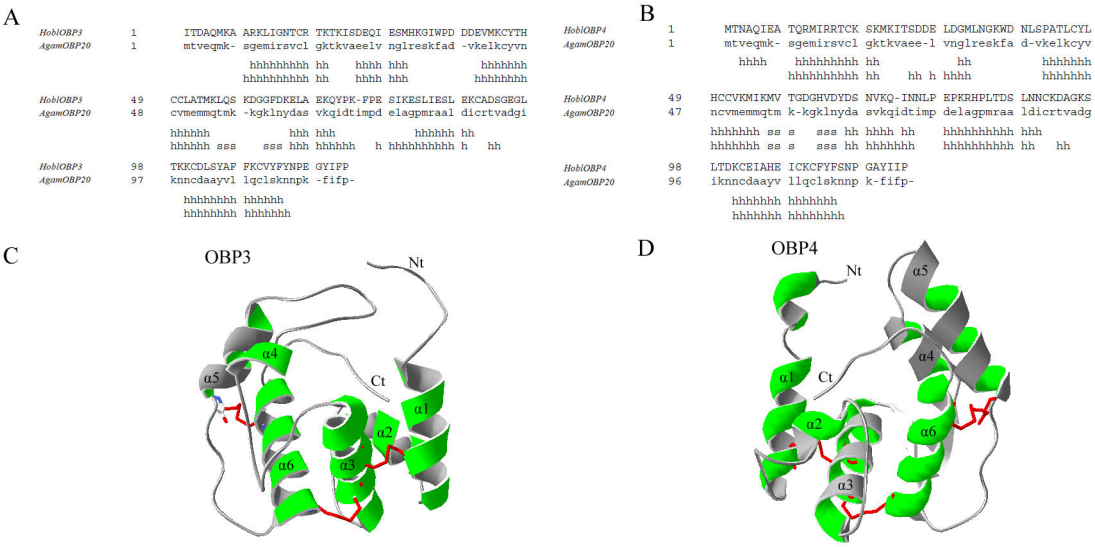

Figure 2. Predicted three-dimensional model of HoblOBP3 and HoblOBP4. Two models both used the crystal structure of *A. gambiae* OBP20 (AgamOBP20) (PDB: 3VB1_A) as a template. (**A**–**B**): Alignments between HoblOBP3 and AgamOBP20 (**A**) or HoblOBP4 and AgamOBP20 (**B**) used in the homologous modeling. The secondary structure elements are shown in the sequence alignments. A small letter "h" in the alignment below the amino acid residues represents the potential α-helix formation. A small letter "s" in the alignment represents the β-sheet formation. (**C**-**D**): the three-dimensional structure of HoblOBP3 (**C**) and HoblOBP4 (**D**) are colored green. The three disulfide bridges are colored red. The N- termini and C- termini as well as α-helices are labeled.

doi: 10.1371/journal.pone.0084795.g002

alignments (Figure 1E). These results demonstrated the diversity of the HoblOBP family.

2 Protein structural analysis

The BLAST analysis was performed against the PDB database to identify suitable templates for the generation of the three-dimensional structures of HoblOBP3 and HoblOBP4. The crystal structure of *A. gambiae* OBP20 (AgamOBP20) (PDB: 3VB1_A) was chosen as a template for both HoblOBP3 and HoblOBP4 [57] The sequence identities between HoblOBP3 and AgamOBP20 and between HoblOBP4 and AgamOBP20 were 26.0% and 26.6%, respectively (Figure 2A-B). The three-dimensional models of HoblOBP3 and HoblOBP4 were predicted using the SWISS-MODEL online tools (Figure 2C-D) [58]. The rationale underlying the model evaluation was based on Ramachandran plot. We found that 82.6% and 14.7% of the HoblOBP3 residues were in the most favored regions and in additional allowed regions, respectively. Moreover, 85.5% and 11.8% of the HoblOBP4 residues were in the most favored regions and in additional allowed regions, respectively.

The predicted three-dimensional structure of HoblOBP3 and HoblOBP4 consisted of six α-helices and three disulfide bridges, which were paired by six conserved cysteines in an interlocking fashion. In the HoblOBP3 pattern, Cys18-Cys50 connected α1-α3, Cys46-Cys102 connected α3-α6 and Cys91-Cys111 connected α5-α6, while for HoblOBP4, Cys18-Cys51 connected α1-α3, Cys47-Cys103 connected α3-α6 and Cys92-Cys112 connected α5-α6 (Figure 2/C-D). The three-dimensional model of HoblOBP3 and HoblOBP4 presented a large binding pocket, and the C-termini extended into the binding pocket, which included the hydrophobic and hydrophilic residues.

3 Expression and purification of the recombinant proteins

Six recombinant *H. oblita* proteins, including HoblOBP1, HoblOBP2, HoblOBP3, HoblOBP4, HoblCSP1 and HoblCSP2, were expressed in *E. coli* at high yields (more than 20 mg/L). Our recombinant HoblOBP3 and HoblOBP4 proteins were expressed in *E. coli* as inclusion bodies and were solubilized under denatured and reducing conditions, while the other four recombinant proteins were presented in soluble forms. The proteins were then purified using Ni ion affinity chromatography and anion exchange chromatography. The histidine-tag of the recombinant proteins was removed by rEK. SDS-PAGE and Western Blotting were then performed (Figure 3). The purified recombinant proteins were then tested for their binding properties and used in the production of polyclonal antibodies.

4 Fluorescence binding assays

Both of the recombinant OBPs (HoblOBP3 and HoblOBP4) was investigated to measure their affinities to a number of potential ligands. 1-NPN was selected as a fluorescent probe to carry out the fluorescent binding experiments [5,13,14]. The dissociation constants were calculated for HoblOBP3 and HoblOBP4, 1.88 μM and 2.78 μM. In both OBPs, a linear profile was obtained from the Scatchard plot (Figure 4).

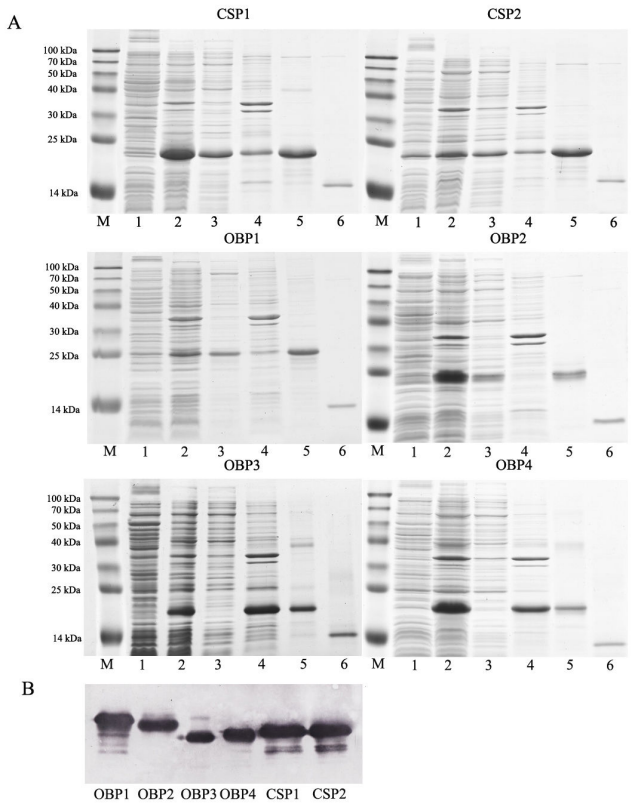

Figure 3. Expression and purification of four OBPs and two CSPs of. *H. oblita*. SDS-PAGE electrophoretic (15% separation gel) (A) and western blotting (B) analysis of expressed recombine proteins. M: Molecular weight marker of 100, 70, 50, 40, 30, 25, 14 kDa; 1-2: before and after induction of the bacterial culture with IPTG; 3: supernatant; 4: inclusion bodies; 5: Purified fusion protein; 6: Purified protein cleaved His-tag by rEK.

doi: 10.1371/journal.pone.0084795.g003

We selected 42 potential organic compounds on the basis of competitive binding assays, which included compounds from volatile green plants, plant odors, attractant compounds of the scarab beetle species and putative sex pheromones of some beetle species (Table 1) [59-61].In particular, these organic compounds were identified on the basis of differences in chain length, functional group and alkene geometry [56]. The IC50 values (the concentration of ligand at half of the initial fluorescence value), the inhibition constants K_i (for each OBP/ligand combination) and the fluorescence intensity (*Int*) (at the ligand concentration (24 μM) represented by the percentage of the initial fluorescence in the absence of a competitor) are summarized in Table 1. Binding curves of a few representative competition experiments (including plant volatiles and putative sex pheromone) are shown in Figure 5.

Similar to related studies performed with other OBPs in the scarab beetle, these two proteins showed clear preferential binding specificities to the ligands examined. While HoblOBP3 appeared to strongly bind to only a few ligands, HoblOBP4 exhibited a broader spectrum of activity and well bound aliphatic and aromatic compounds consisting of 4–13 carbon atoms. The compounds, 1-hexanol, trans-2-hexenal, butyl benzoate, hexyl benzoate and cinnamaldehyde, showed high binding affinities to HoblOBP4 with K_i values of 8.8, 8.1, 8.1, 2.9 and 6.6 μM□respectively, while only α-ionone and β-ionone displayed binding affinities to HoblOBP3 with K_i values of 10.4 and 5.2 μM, respectively. A large number of aliphatic compounds were tested in competition experiments, which revealed moderate binding affinity (Table 1).

Interestingly, good affinities for HoblOBP4 were observed for aliphatic alcohols and aldehydes with carbon numbers of six, particularly those containing an insertion of two double bonds into trans-2-hexenal, which restored high binding activity (Figure 6A). For terpenoids with carbon numbers of ten and an open-chain molecular structure, its affinity was higher than for terpenoids with a ring-shaped structure (Figure 6B). In addition, good affinity for HoblOBP4 was also found in open-chain structure compounds bearing other functional groups, such as a hydroxyl group (Figure 6B). Another remarkable observation involved the enhanced affinity demonstrated by aliphatic ester groups compared to other aliphatic groups, which showed a drastically increased affinity with as the carbon number increased; these groups included propyl benzoate, butyl benzoate and hexyl benzoate (Figure 6C). Putative sex pheromone compounds of some beetle species, such as L-isoleucine methyl ester, R-(-)-linalool and glycine ethyl ester, may bind to HoblOBP4 (Figure 6D).

5 Fluorescence binding assays with binary protein mixtures

It is well known that the concentration of OBPs (also likely CSPs) in the sensillum lymph of the insect is extremely high (reportedly 10 mM) [7]. A hypothesis has been proposed that OBPs (or CSPs) homodimers or heterodimers might form [7,43,44]. Thus, all binary potential intersections with four HoblOBPs and two HoblCSPs were tested in competitive binding assays to determine the existence of dimers. These experiments assumed that the protein was 100% active, a stoichiometric ratio between the protein and ligand was 1:1 at saturation and the two proteins were present in equimolar amounts. The representative binding results of 1-NPN to OBP binary mixtures are shown in Figure 7. The binding curves and Scatchard plots of OBP3 and OBP4 mixture or CSP1 and CSP2 mixture were consistent with the functions of the individual proteins. However, the binding curve of the OBP2 and OBP4 mixture or OBP1 and OBP2 mixture presented a different tendency from those obtained with the individual proteins. Moreover, the Scatchard plot exhibited a “J”-like nonlinear correlation trend. Thus, we speculated that the decreased binding velocity was the main cause underlying this phenomenon. When one of the binary protein mixtures demonstrated a good affinity, it would first bind to the fluorescent probe 1-NPN and initially display a rapid upstroke on the binding curve diagram. In contrast, the other proteins from the mixture that exhibited weak binding affinity to 1-NPN and a delayed binding velocity, showed a downward trend at higher concentrations on the binding curve diagram. Such

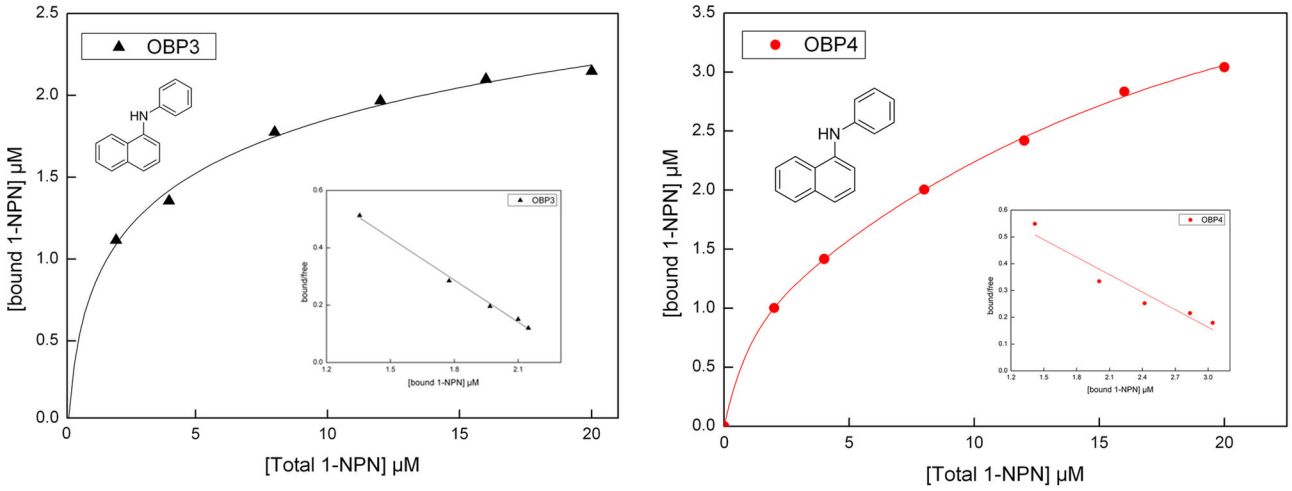

Figure 4. Binding curves of 1-NPN and the relative Scatchard plot. A solution of the protein with 2 μM in Tris-buffer was titrated with 1 mM solution of 1-NPN in methanol, with final concentrations of 2–20 μM. Dissociation constants were HoblOBP3: 1.88 μM; HoblOBP4: 2.78 μM.

doi: 10.1371/journal.pone.0084795.g004

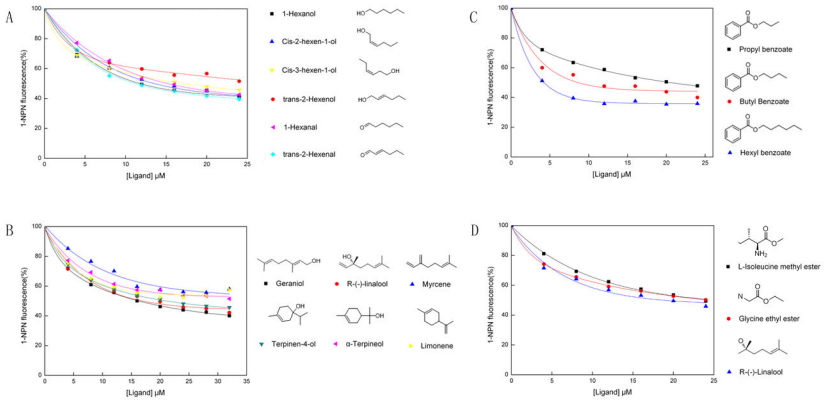

Figure 6. Competitive binding curves of characteristic ligands to recombinant HoblOBP4. The chemical structures of the ligands are shown on the right. (**A**) Competitive binding curves of aliphatic alcohols and aldehydes with six carbon numbers. (**B**) Competitive binding curves of different structural on terpenoids with ten carbon numbers. (**C**) Competitive binding curves of aliphatic ester with different carbon numbers. (**D**) Competitive binding curves of the sex pheromone component.

doi: 10.1371/journal.pone.0084795.g006

binding of the OBP2 and OBP4 mixture or OBP1 and OBP2 mixture in *H. oblita* was consistent with the OBP1 and OBP4 mixture in *A. gambiae* [44]. In particular, some experiments also indicated interactions between OBP1 and OBP4 in *A. gambiae* [43]. Thus, the hypothesis on a potential interaction between OBP2 and OBP4 (or OBP1 and OBP2) in *H. oblita* was proposed.

We selected four representative organic compounds, including β-ionone, cinnamaldehyde, eugenol and retinol, on the basis of the results obtained from the competitive binding assays with OBP2 and OBP4 mixtures in *H.oblita* (Figure 8). Cinnamaldehyde, eugenol and retinol have been previously reported to demonstrate low-affinity or non-affinity, and β-ionone has been shown to exhibit good affinity for HoblOBP2 [13]. In contrast, cinnamaldehyde and β-ionone showed good affinity, and the remaining two compounds showed no affinity for HoblOBP4 in our study. When we investigated the HoblOBP2 and HoblOBP4 mixtures, we found the good affinity exhibited on these four compounds. β-ionone displayed an enhanced affinity with OBP2 and OBP4 mixtures compared to the individual protein. Surprisingly, good affinity was measured for retinol with HoblOBP2 and HoblOBP4 mixtures, which extremely differed from the individual protein (neither HoblOBP2 nor HoblOBP4 could bind to retinol alone). This result indicated that retinol could bind in a heterodimeric manner with OBP2/OBP4 in *H. oblita*.

Table 1. Binding of pure organic compounds to selected recombinant OBPs of *H. oblita*.

Ligands	HoblOBP3			HoblOBP4		
	IC50	*Int*	K_i	IC50	*Int*	K_i
Aliphatic alcohols						
1-Hexanol	-	91	-	12	45	8.8
trans-2-Hexenol	-	82	-	24	51	17.7
cis-2-Hexen-1-ol	-	70	-	14	42	10.3
cis-3-Hexen-1-ol	-	81	-	17	46	12.5
1-Heptanol	-	70	-	21	46	15.4
1-Octen-3-ol	-	86	-	40	54	29.4
1-Nonanol	-	71	-	16	46	11.8
4-tert-Butyl cyclohexanol	-	68	-	19	49	14.0
Retinol	-	-	-	-	-	-
Aliphatic aldehydes						
1-Pentanal	41	65	26.8	16	44	11.8
1-Hexanal	-	68	-	15	42	11.0
trans-2-Hexenal	-	74	-	11	39	8.1
1-Heptanal	-	65	-	-	64	-
1-Decanal	-	86	-	-	68	-
Aliphatic ketones						
2-Cyclohexen-1-one	-	70	-	23	49	16.9
6-Methyl-5-hepten-2-one	-	78	-	32	52	23.5
Aliphatic alkanes						
Heptane	-	63	-	16	43	11.8
Octane	-	70	-	25	51	18.4
Nonane	-	-	-	-	-	-
Decane	-	-	-	-	-	-
Aliphatic ester						
Glycine ethyl ester	-	76	-	24	50	17.6
L-Isoleucine methyl ester	-	68	-	24	49	17.7
L-Proline ethyl ester	-	70	-	20	47	14.7
(Z)-3-Hexenyl acetate	-	78	-	40	56	29.4
Propyl benzoate	-	81	-	20	48	14.7
Butyl Benzoate	-	69	-	11	40	8.1
Hexyl benzoate	-	53	-	4	36	2.9
Terpenoids						
Geraniol	-	79	-	16	44	11.8
R-(-)-Linalool	-	73	-	20	46	14.7
Myrcene	-	74	-	-	56	-
Terpinen-4-ol	-	75	-	21	48	15.4
α-Terpineol	-	71	-	35.5	53	26.1
Limonene	-	56	-	-	52	-
α-Ionone	16	41	10.4	19	45	14.0
β-Ionone	8	36	5.2	15	42	11.0
β-Caryophyllene	-	-	-	-	-	-
Aromatic compounds						
Benzaldehyde	-	68	-	17	44	12.5
Phenethyl alcohol	-	66	-	28	52	20.6
Menthyl salicylate	-	75	-	-	54	-
Benzeneacetaldehyde	-	-	-	-	-	-
Cinnamaldehyde	46	64	30.0	9	36	6.6
Eugenol	-	97	-	-	57	-

A similar assay was performed in HoblOBP1 and HoblOBP2 mixtures with trans-2-hexenol, 1-heptanal, R-(-)-linalool and α-

Table 1 (continued).

Solution of protein and 1-NPN, both at concentration of 2 μM, was in line with the dissociation constants of HoblOBPs/1-NPN complex calculated. Then the mixed solution was titrated with 1 mM solution of each ligand in methanol to final concentrations of 2–50 μM. For each protein, we report the fluorescence intensity (*Int*) measured at the ligand concentration (24 μM) as percent of the initial fluorescence, the concentration of ligand halving the initial fluorescence intensity (IC50), where applicable, and the relative dissociation constant (K_i) calculated as described in ''Materials and methods''. Dissociation constants of ligands whose IC50 exceeded 50 μM are represented as ''-''.

doi: 10.1371/journal.pone.0084795.t001

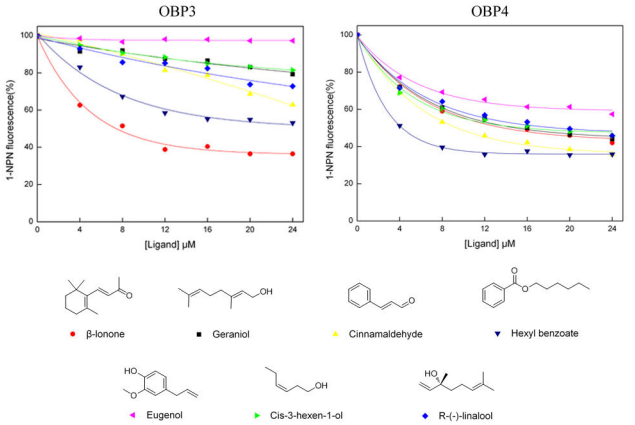

Figure 5. Competitive binding curves of representative ligands to recombinant HoblOBP3 and HoblOBP4. The chemical structures of the ligands are shown below. A mixture of the protein and 1-NPN with both concentration of 2 μM in Tris-buffer was titrated with 1 mM solution of each competing ligand to final concentrations of 4–24 μM.

doi: 10.1371/journal.pone.0084795.g005

terpineol (Figure 8). Competitive binding assays of HoblOBP1 or HoblOBP2 alone with these four compounds have been previously tested, which showed low-affinity or non-affinity, respectively [13]. Interestingly, an enhanced affinity on HoblOBP1 and HoblOBP2 mixtures compared to HoblOBP1 or HoblOBP2 alone was observed in these four compounds, which was consistent with the results of the HoblOBP2 and HoblOBP4 mixtures.

6 Colocalization immunocytochemistry

Double-labeling for HoblOBP1 and HoblOBP2 (Figure 9) and for HoblOBP2 and HoblOBP4 (Figure 10) was performed using colloidal gold post-embedding immunocytochemistry. Polyclonal antiserums of HoblOBPs (anti-OBP1, anti-OBP2, and anti-OBP4) were used to determine the cellular localization of HoblOBPs in the adult antennae. For double-labeling of HoblOBP1 and HoblOBP2, anti-OBP1 was labeled using a 10-nm gold marker (large silver-intensified granules), and anti-OBP2 was labeled using a 5-nm gold marker (small silver-

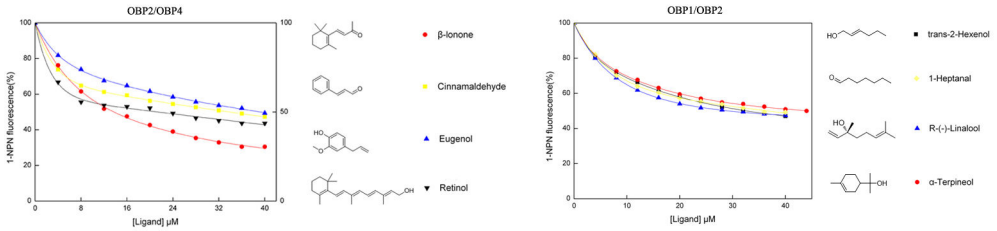

Figure 8. Competitive binding curves of representative ligands to binary protein mixtures OBP2-OBP4 and OBP1-OBP2 in. *H. oblita*. The chemical structures of the ligands are shown on the right. A mixture of the proteins (equimolar amounts) and 1-NPN with both concentration of 2 μM in Tris-buffer was titrated with 1 mM solution of each competing ligand to final concentrations of 4–40 μM.

doi: 10.1371/journal.pone.0084795.g008

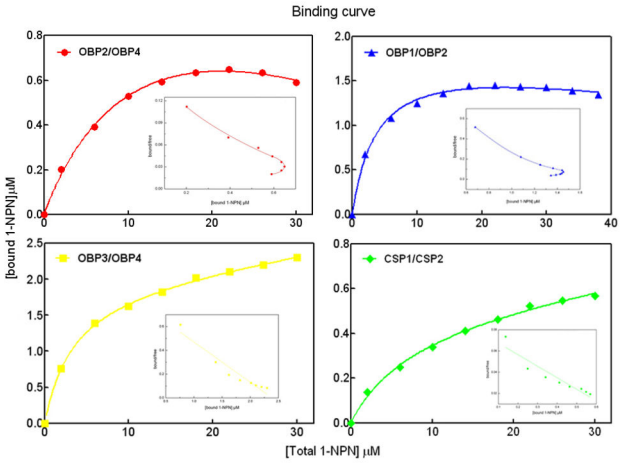

Figure 7. Binding curves of 1-NPN and the relative Scatchard plot using binary protein mixtures. A solution of the protein mixtures (1:1) with 2 μM in Tris-buffer was titrated with 1 mM solution of 1-NPN in methanol, with final concentrations of 2–30 μM.

doi: 10.1371/journal.pone.0084795.g007

intensified granules), which are shown in Figure 9B, D, E, and F. Similarly, the double-labeling of HoblOBP2 and HoblOBP4 are shown in Figure 10B, D, E, and F. Different chemosensory sensilla, sensilla placodea (Figure 9 and 10A, B, and E) and sensilla basiconica (Figure 9 and 10C, D, and F) of both sexes were strongly labeled by the two protein groups (HoblOBP1 and HoblOBP2 or HoblOBP2 and HoblOBP4), suggesting that each protein group was coexpressed in these same sensilla. The outer sensillum lymph (osl) surrounding the dendrites (d) was robustly labeled (Figure 9 and 10A–D), while the inner sensillum lymph (isl) of the dendrites was never labeled (Figure 9 and 10A, C).

Discussion

Full-length cDNAs encoding HoblOBP3 and HoblOBP4 were cloned using RACE-PCR. The deduced amino acid sequence suggested that these two proteins consisted of a typical framework of OBPs (six-conserved cysteines) and may be new members of the OBP family in *H. oblita* but share a low sequence similarity from other species of Coleoptera, including HoblOBP1 and HoblOBP2. In fact, Coleoptera is the biggest order in insecta. However, reported OBPs in Coleoptera are very rare. Since the first genome sequences of the red flour beetle *T. castaneum* has been sequenced [55], a growing number of OBPs have been found in Coleoptera [13,52] and more will surely be discovered and their diversified functions revealed in the future.

Our fluorescent binding experiments provided interesting results. In general, HoblOBP4 exhibits a broader affinity compared to HoblOBP3 in response to the ligands assayed. Such binding specificity of HoblOBP3 with α-ionone and β-ionone is remarkable when compared with the broad spectrum of binding to other insect OBPs, as previously reported in the literature [12-14], While HoblOBP4 demonstrated a broader spectrum of activity, it exhibited good binding with aliphatic and aromatic compounds containing 4–13 carbon atoms, particularly with hexyl benzoate. Interestingly, we observed an enhanced affinity of HoblOBP4 for aliphatic esters compared to other aliphatic groups; its affinity increased drastically as the carbon number increased (i.e., propyl benzoate, butyl benzoate and hexyl benzoate). These results were consistent with previous reports of HoblOBP1 and HoblOBP2 [13]. In our binding assay, β-ionone, a strong ligand, showed a higher affinity compared to α-ionone for both HoblOBP3 and HoblOBP4, which suggests that isomers constitute one factor that influence affinity in fluorescence binding experiments. In another analysis of our experiment, the effect on the length difference of the carbon chains was reflected in the binding affinity. In general, the ligand affinities decreased when the number of carbon atoms increased, which was mainly observed in the aliphatic alkanes. Moreover, good affinity was measured for aliphatic alcohols and aldehydes with carbon numbers of six in HoblOBP4, particularly the insertion of two double bonds in the trans-2-hexenal, which restored high binding activity. For terpenoids with carbon numbers of ten, its affinity for an open-chain molecular structure was higher compared to that for terpenoids with a ring-shaped structure. In addition, good affinity was also observed with open-chain structure compounds bearing other functional groups, such as a hydroxyl group. Thus, the good affinity observed in geraniol

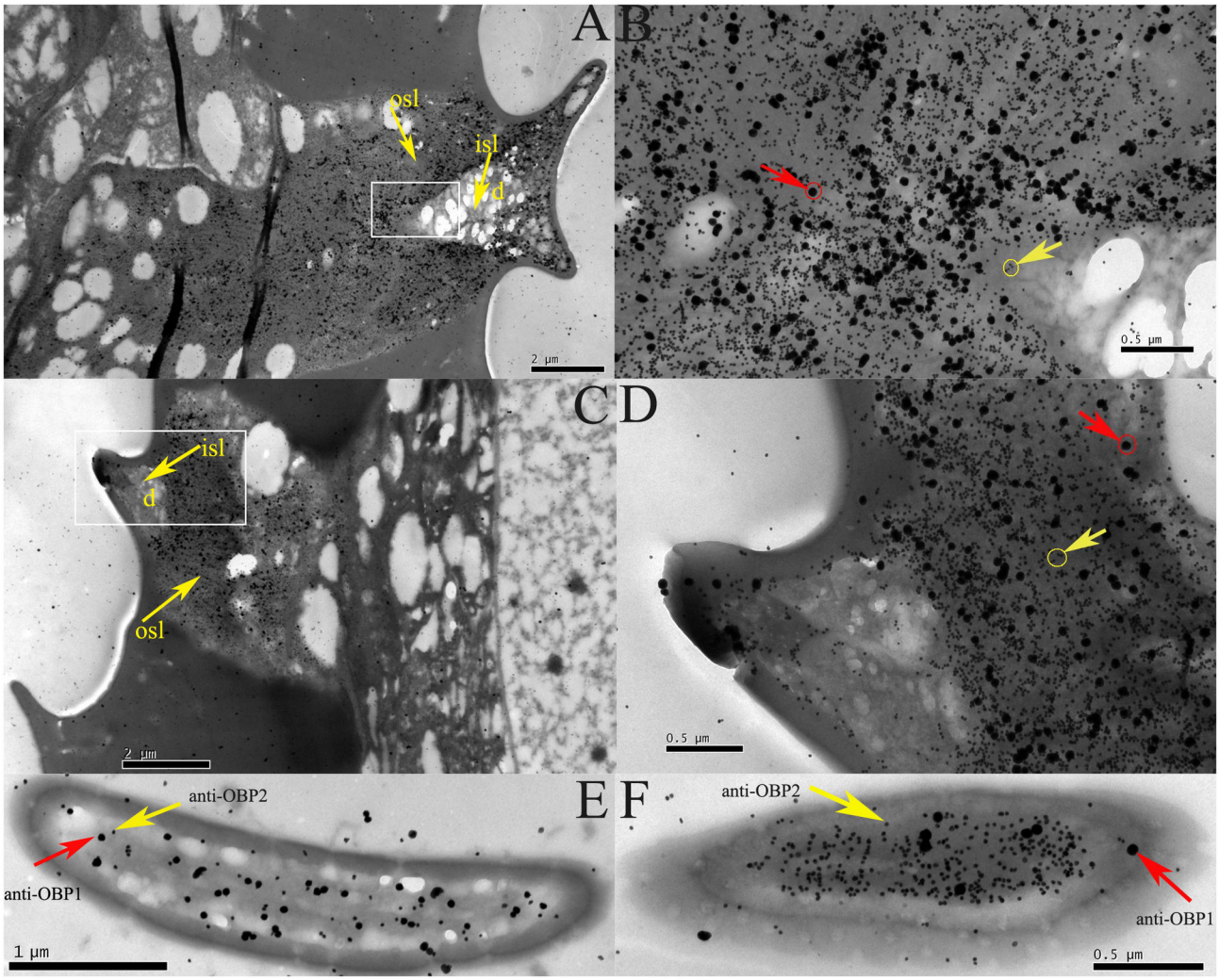

Figure 9. Immunocytochemical colocalization of OBP1-2 in the olfactory sensilla of adult. *H. oblita*. The coexpressed of HoblOBP1-2 in Sensilla placodeum (A, B, and E) and Sensilla basiconica (C, D, and F) was detected by double labelling of colloidal gold immunocytochemistry. The anti-OBP1 was labeled by the 10-nm gold marker (large silver-intensified granules, with red arrows in B, D, E, and F) and anti-OBP2 was labeled by 5-nm gold marker (small silver-intensified granules, with yellow arrows in B, D, E, and F). B and D was enlargement of part of A and C in white pane respectively. Inner (isl) and outer (osl) sensillum lymph of the dendrites (d) was marked with yellow arrows in A and C.

doi: 10.1371/journal.pone.0084795.g009

can be easily explained. Furthermore, cinnamaldehyde exhibits good affinity, which may be attributed to its functional groups (the presence of double bonds or an aldehyde group). In contrast, β-caryophyllene exhibited a much weaker affinity, which could be attributed to its large ring structure. Thus, the position and variety of functional groups may considerably affect the binding affinity. Briefly, our fluorescent binding experiments were consistent with other previously reported insect OBPs, and chain length, functional group and alkene geometry were the main impact factors that affected binding affinity [5,12-14,56].

In our study, the three-dimensional structure of HoblOBP3 and HoblOBP4 was predicted respectively. The crystal structure of AgamOBP20 was selected as the template for both HoblOBP3 and HoblOBP4 [57]. It has been shown that its C-terminus folds back into the protein core, which was similar in structure to AgamOBP1 [37]. Such a conformation is similar to the structures of other OBPs, which have been previously published in the honeybee *Apis mellifera* (AmelASP1), mosquito *A. aegypti* (AaegOBP1), and mosquito *C. quinquefasciatus* (CquiOBP1) [38,39,62]. However, these OBPs did not form a seventh α-helix in the C-terminus and have different binding mechanisms in the silkworm *B. mori* PBP [6]. It may be assumed that if similar structures correspond to the same mechanism of binding and releasing, then HoblOBP3 or HoblOBP4 will be consistent with these OBPs. Moreover, we

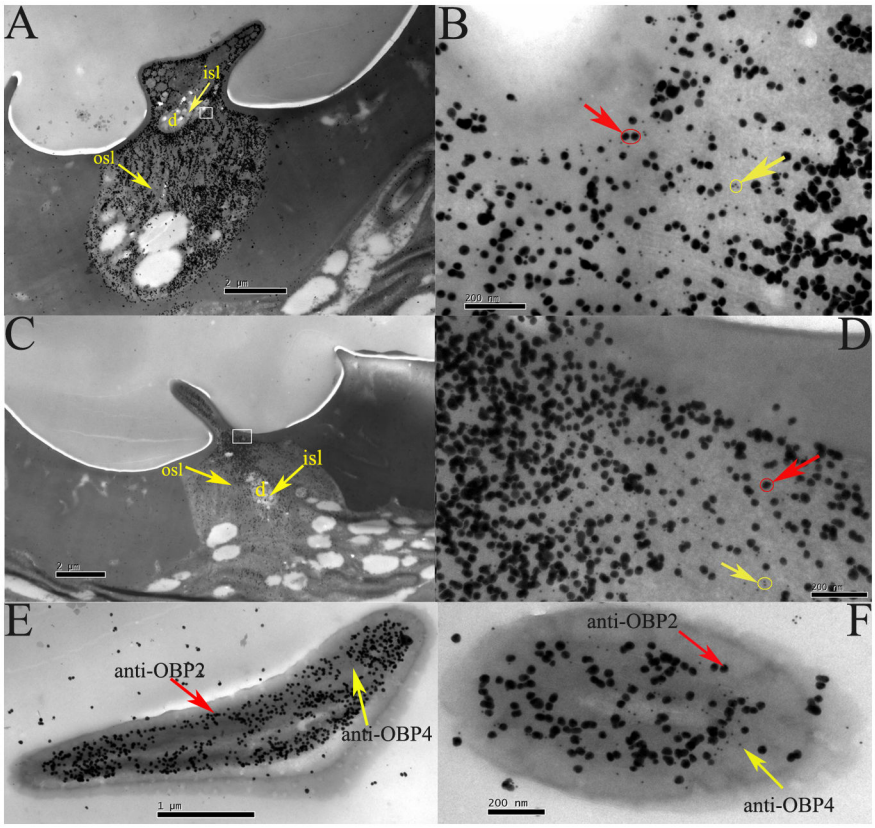

Figure 10. Immunocytochemical colocalization of OBP2-4 in the olfactory sensilla of adult. *H. oblita*. The coexpressed of HoblOBP2-4 in Sensilla placodeum (A, B, and E) and Sensilla basiconica (C, D, and F) was detected by double labelling of colloidal gold immunocytochemistry. The anti-OBP2 was labeled by the 10-nm gold marker (large silver-intensified granules, with red arrows in B, D, E, and F) and anti-OBP4 was labeled by 5-nm gold marker (small non-intensified granules, with yellow arrows in B, D, E, and F). B and D was enlargement of part of A and C in white pane respectively. Inner (isl) and outer (osl) sensillum lymph of the dendrites (d) was marked with yellow arrows in A and C.

doi: 10.1371/journal.pone.0084795.g010

also predicted the three-dimensional structure of HoblOBP1 and HoblOBP2, which were similar to HoblOBP3 and HoblOBP4. The related analysis of ligands binding site with these HoblOBPs will be issued in another paper (Zhuang XJ et al, in preparation). It will further explain the interacted mechanism between ligands and proteins.

An alternative hypothesis that has been proposed involves the protein-binding pocket and its ability to form a long hydrophobic tunnel from one end of the protein to the other (present as a dimer), which may potentially allow ligands to freely pass through the protein channel [37]. Given the exceptionally high concentration (10 mM) reported for OBPs in the sensillar lymph with individual proteins that nearly touching one another, it is likely that the hydrophobic ligand could pass from one OBP to other until it reaches to the ORs [7]. This model, which is suggested by the AgamOBP1 structure, is presented as a dimer [37]. In the same year, another study on specific interactions among odorant-binding proteins of *A. gambiae* has demonstrated that two OBPs, OBP1 and 4, are capable of forming heterodimers [43]. Subsequently, another study also indicated that the unexpected binding characteristics of AgamOBP1 and AgamOBP4 mixtures, as measured using fluorescence binding assays, could be interpreted as the heterodimeric formation of OBPs [44]. All of these studies provide convincing evidence for a hydrophobic tunnel hypothesis. Interestingly, HoblOBP1 and HoblOBP2 are structurally analogous to AgamOBP1 (unpublished data), and our experimental results demonstrate that the binding characteristics of HoblOBP1 and HoblOBP2 mixtures, as measured using fluorescence binding assays, are consistent with the AgamOBP1 and AgamOBP4 mixtures, which exhibit an unusual tendency. The competitive binding assays of HoblOBP1 and HoblOBP2 mixtures were performed with some representative organic compounds. These results show that an enhanced affinity is exhibited in HoblOBP1 and HoblOBP2 mixtures compared to either HoblOBP1 or HoblOBP2 alone. Moreover, parallel colocalization analysis indicated that OBP1 and OBP2 are co-expressed in the same sensilla. Thus, potential dimer formation between HoblOBP1 and HoblOBP2 has been proposed to support the hypothesis of a long

hydrophobic tunnel in *H. oblita*. Such a presumption may also be pertinent for the dimer formation between HoblOBP2 and HoblOBP4 and may be another piece of evidence supporting good affinity for retinol in HoblOBP2 and HoblOBP4 mixtures, although retinol demonstrated good affinity with neither HoblOBP2 nor HoblOBP4 alone. It is suggested that retinol might be bound by the heterodimeric OBP2/OBP4 in *H. oblita*. In the general case, the binding affinities of these ligands decreased when the number of carbon atoms increased [13,14]. If so, it is possible that the recognition mechanism of the insect for multi-carbon macromolecular compounds may be realized by dimer transportation. We deduce that HoblOBP2 and HoblOBP4 form heterodimers, while HoblOBP1 formed homodimers in the former study [13]. Similar to the hypothesized hydrophobic protein tunnel in AgamOBP1, it is likely that a long hydrophobic tunnel consisting of OBP heterodimers or homodimers will transport the ligand to the ORs if an identical ligand can be recognized from multiple HoblOBPs.

In this study, coexpression was observed at the subcellular level by immunocytochemical localization of two OBP groups within the *H. oblita* antennae. Importantly, a large number of studies on OBPs using polyclonal antibodies were performed in Lepidoptera. As a general rule, the sensilla trichodea express PBPs, while most sensilla basicona, which respond to general odorants, mainly express GOBPs [63-66]. However, a colocalization study performed in the same sensillum was completed using two OBPs of *Drosophila*: OS-E and OS-F [67]. The resulting study confirmed three Drosophila OBPs (LUSH, OS-E and OS-F), which were coexpressed in the sensilla trichodea, using colloidal gold post-embedding immunocytochemistry [68]. Similar conclusions regarding their colocalization were confirmed in *A. gambiae* OBPs [44]. In a previous study of OBPs in *H. oblita*, consecutive sections labeled with anti-OBP1 and anti-OBP2 antisera, respectively, illustrated that HoblOBP1 and HoblOBP2 were both expressed in the sensilla placodea and basiconica [13]. Colloidal gold granules of different sizes were used to confirm the colocalization of HoblOBP1 and HoblOBP2 in the same sensillum. Such circumstances also apply to HoblOBP2 and HoblOBP4. Importantly, HoblOBP1 and HoblOBP2, as well as HoblOBP2 and HoblOBP4, are co-expressed in sensilla placodea and basiconica, respectively, which are likely to shift toward the functional relevance of heterodimers in the sensillum lymph. It has been suggested that the co-expression of different OBPs within the same sensillum may potentially broaden the range of odorants to which the olfactory receptor neurons can respond [13,69]. Thus, the colocalization between HoblOBPs strongly supports the hydrophobic tunnel hypothesis.

Our binding assay and colocalization studies support that OBPs can effectively perceive plant volatiles or pheromones by forming heterodimers in the sensillum lymph and potentially expanding their chemical communication, which are consistent with hydrophobic tunnel hypothesis. Thus far, several types of mechanisms underlying olfactory recognition have been proposed to explain the insect's physiological functional and behavioral responses. All of these hypotheses contribute to a better understanding of olfactory processes in insects, which can facilitate the development of strategies directed towards disrupting specific behaviors in pest species.

Materials and Methods

1 Insects and reagents

The scarab beetle *H. oblita* was provided by Cangzhou Academy of Agriculture and Forestry Sciences, Cangzhou city, Hebei province, China. When the scarab beetle breaks out, it was collected in the test field from Cangzhou Academy of Agriculture and Forestry Sciences. This collection of *H. oblita* is permitted by the committee of Biology of Plant Diseases and Insect Pests of Cangzhou Academy of Agriculture and Forestry Sciences. The adult antennae were dissected in 0.75% NaCl saline solution and immediately frozen in liquid nitrogen. The isolated antennae were stored at –70°C until use.

2 Screening of OBP genes in the antennal cDNA library

Total antennal RNA was isolated from 100 antennae of *H. oblita* (females) using Trizol reagent (Invitrogen, Carlsbad, CA, USA). The antennal cDNA library was constructed using the Creator™ SMART™ cDNA Library Construction Kit (Clontech, Mountain, CA, USA), according to the manufacturers' protocol. Single clones were picked and sequenced after being inserted into a vector (TaKaRa Co., Dalian, China). The partial sequences of the OBP genes were identified using BlastX.

3 Cloning and sequencing

The overall lengths of the cDNA sequences were obtained by performing rapid-amplification of cDNA ends (RACE), according to the instructions of the 5'- Full RACE Kit and 3'-Full RACE Core Set Ver.2.0 (Takara Co., Dalian, China). The 5' and 3' RACE gene-specific primers (GSPs) were designed from the partial coding sequences of HoblOBP3 and HoblOBP4 and synthesized by TaKaRa Company (Dalian, China). These primer sequences are listed in Table 2. Polymerase chain reaction (PCR) was performed using ExTaq DNA polymerase (Takara Co., Dalian, China) under the same conditions, including a pre-denaturation step (94°C for 3 min), 30 cycles (94°C for 30 s, 55°C for 30 s and 72°C for 1 min) and further extension (72°C for 10 min). The PCR products were digested and ligated into the pGEM-T Easy Vector (Promega, Madison, WI). The recombinant plasmid was transformed into *E. coli* DH5α competent cells and plated onto LB solid medium/ ampicillin. Positive clones were selected for the sequence using the dideoxynucleotide chain termination method (TaKaRa Co., Dalian, China).

4 Sequences and structural analysis

When complete the coding sequences of HoblOBP3 and HoblOBP4 obtained using the RACE method, the open reading frames (ORFs) were deduced using the Open Reading Frame Finder (http://www.ncbi.nlm.nih.gov/gorf/gorf.html). The putative signal peptides were predicted using the SignalP 4.1 Server [70]. The molecular weights of the proteins were predicted using SWISS-PROT (http://www.expasy.org/

Table 2. Oligonucleotide primers used for amplifying OBP3 and OBP4 genes in *H. oblita*.

Protein category	Primer name	Sequence
OBP3	3' RACE GSP1	5' -CCAGATGATGACGAAGTTATGAAG-3'
	3' RACE GSP2	5' -TACACGCACTGTTGCCTGG-3'
	5' RACE GSP1	5' -CCTTCACCAGAGTCAGCGCAT-3'
	5' RACE GSP2	5' -ATTCTTTATCAAAACCTCCATC-3'
	Forward(partial)	5' -ATAACTGATGCCCAAATGAT-3'
	Reverse(partial)	5' -TGGGAATATATAGCCTTCTGGATTG-3'
	Forward	5' -GAATTCATGATGAAAGTTCCGTTAGTG
	Reverse	5' -CTCGAGTCATGGGAATATATAGCCTTCTGGA
OBP4	3' RACE GSP1	5' -CTAAGCCCCGCTACTTTGTGTT-3'
	3' RACE GSP2	5' -CAAAATGGTTACAGGAGATGG-3'
	5' RACE GSP1	5' -CGACTTTCCTGCATCTTTAC-3'
	5' RACE GSP2	5' -TGGCGCTTTGGCTCTGGTAA-3'
	Forward(partial)	5' -ATGACCAACGCTCAGATTG-3'
	Reverse(partial)	5' -GGTATAATATAAGCTCCAGGATTA-3'
	Forward	5' -GAATTCATGACCATGTTCTTATATTTTC
	Reverse	5' -CTCGAGTTACGGTATAATATAAGCTCCAG

GAATTC and CTCGAG presents restriction enzyme cutting site, EcoRI and XhoI, respectively.

doi: 10.1371/journal.pone.0084795.t002

compute_pi). Several OBP sequences of Coleopteran insects were downloaded from the GenBank sequence database and aligned using CLUSTALX 2.0.7[71]. The phylogenetic tree was constructed with MEGA 4.0 (using a neighbor-joining method), and the samples were bootstrapped 1000 times [72].

Three-dimensional models of HoblOBP3 and HoblOBP4 were predicted using the SWISS MODEL on-line tools (http://swissmodel.expasy.org/) [73]. Both HoblOBPs were used on the basis of the structure with the highest alignment score as a template to construct three-dimensional models. Models were manipulated using the Swiss-Pdb Viewer 4.1.0 Server [73]. The rationale underlying the established model evaluation was based on a Ramachandran plot [74].

5 Recombinant expression and purification

Gene-specific primers were designed to clone the coding regions of HoblOBP3 and HoblOBP4. The related specific primers with XhoI and EcoRI restriction enzymes site are listed in Table 2. The coding nucleotide sequences were first cloned into the pGEM-T easy vector (Promega, Madison, WI) and digested by XhoI and EcoRI enzymes. The digested products were then ligated into the pET30a (+) expression vector (Novagen, Madison, WI) and verified by sequencing. Plasmids containing the correct insert (pET30a-HoblOBPs) were then transformed into *E.coli* BL21 (DE3) pLysS competent cells. A single clone of pET30a-HoblOBPs was identified by PCR and sequencing.

In addition to pET30a-HoblOBP3 and pET30a-HoblOBP4, we also selected four other recombinant plasmids (curated in our lab) including pET30a-HoblOBP1, pET30a-HoblOBP2, pET30a-HoblCSP1 and pET30a-HoblCSP2. All six recombinant plasmids were transformed into *E. coli* BL21 (DE3) pLysS cells and induced with isopropyl-beta-D-thiogalacto-pyranoside (IPTG) at a final concentration of 0.7 mM at 28°C for 8 hours. The samples were sonicated and centrifuged at a low temperature, and the supernatant and pellet were analyzed using sodium dodecyl sulfate polyacrylamide gel electrophoresis (SDS-PAGE). HoblOBP3 and HoblOBP4 were found as inclusion bodies, while the other plasmids were expressed in the supernatant. Soluble proteins were purified using Ni ion affinity chromatography (GE-Healthcare Biosciences, Uppsala, Sweden) for His-tagged-protein purification and anion exchange chromatography (GE Healthcare Biosciences, Uppsala, Sweden). The inclusion body proteins were purified under denaturing conditions (dissolved in 6 M guanidinium hydrochloride buffer) according to previously described redox protocols [56]. Recombinant enterokinase (rEK) (Bio Basic Inc.) was used to remove the His-tag. A second round of Ni ion affinity chromatography was performed to obtain the purified proteins. Next, the proteins were concentrated using Amicon Ultra concentrators with a 10 kDa cutoff (Millipore) and confirmed using SDS-PAGE analysis. The concentrations of the six proteins were then measured using the Bradford method with BSA as the standard protein [75].

6 Western blotting analysis

After protein electrophoresis under denaturing conditions (15% SDS-PAGE gel), duplicate gels were prepared for Analysis. 1 gel was stained with 0.1% Coomassie brilliant blue R-250 (in 10% acetic acid, 45% methanol), while the other gel was electrophoresed onto a piece of nitrocellu-lose membrane (Millipore, USA) [5]. After electrophoresis, the membrane was incubated with 5% powdered skimmed milk (0.05% Tween 20 in TBS) overnight. Next, monoclonal mouse anti-His tag fusion protein (California Bioscience, USA) at a dilution of 1:1000 (2 hours) and goat anti-mouse IgG with an alkaline phosphatase labeled (Sigma Aldrich, USA) at a dilution of 1:1000 (1 hour) were incubated sequentially. Immunoreactive bands were detected using 5-bromo-4-chloro-3-indolyl phosphate (BCIP, 0.15 mg/ml) and nitrotetrazolium blue chloride (NBT, 0.3 mg/ml) at a ratio of 1:2.

7 Preparation of the antisera

Antisera were obtained by subcutaneously injecting an adult mouse with 50 μg of recombinant HoblOBP3 or HoblOBP4 protein, followed by 3 additional injections of 25 μg on the 21st, 35th, and 49th day. Four mice were used in a parallel study. The proteins were emulsified with an equal volume of Freund's complete adjuvant on the first injection and Freund's incomplete adjuvant on the second injection. The antiserum was then tested using an enzyme-linked immunosorbent assay. The mice were exsanguinated 10 days after the last injection, and the serum was used without further purification. Other HoblOBPs antisera were obtained by injecting adult rabbits.

8 Ethic statement

I proclaimed that the following statement was accurate. All animal procedure in this study was strictly performed according

to guidelines developed by the ethics committee of the State Key Laboratory for Biology of Plant Diseases and Insect Pests, Institute of Plant Protection, Chinese Academy of Agricultural Sciences. The approval ID or permit numbers is SYXK (Beijing) 2008-008. All animal procedure was performed under anesthesia, and wounds were cleaned that before they got infected. All efforts were made to minimize suffering.

9 Fluorescence binding assays

N-phenyl-1-naphthylamine (1-NPN) was selected as a probe to measure the affinity of the 1-NPN fluorescent ligand to proteins [5,13,14]. A 1-cm light path quartz cuvette was used, and the fluorescence spectra were recorded on a Lengguang 970 CRT spectrofluorimeter (Shanghai Jingmi, China) at room temperature in a right angle configuration. The parameter selection was such that the slit widths for both excitation and emission were 10 nm. 1-NPN was excited at 337 nm and the emission spectra were recorded between 350 and 550 nm. Spectra were recorded using high-speed scanning. Several types of compounds purchased from Sigma-Aldrich (Chemie Gmbh, Steinheim, Germany) were identified in the binding assays, and their purities were > 97% (Table 1).

The 2 μM protein solution was dissolved in 50 mM Tris-HCl buffer with pH 7.4, and the ligands were dissolved in chromatographically pure methanol as a 1 mM stock solution. 1-NPN was dissolved in chromatographically pure methanol as a 1 mM stock solution. The protein solution was titrated to measure the protein's affinity for the probe by adding aliquots of 1-NPN stock solution to final concentrations of 2 to 20μM. The affinity of the ligands was estimated using competitive binding assays with both 1-NPN and proteins at 2 μM; the final concentrations for each competitive ligand were in the range of 2 to 24 μM.

To determine the dissociation constants, the intensity values corresponding to the maximum fluorescence emission were plotted against free ligand concentrations. Assuming that the protein was 100% active and that the stoichiometric ratio between the protein and ligand was 1:1 at saturation, the bound ligand was determined from the fluorescence intensity values. The curves were then linearized using Scatchard plots. The $K_{1\text{-NPN}}$ values were estimated using GraphPad Prism 5 Software by nonlinear regression for a unique binding site [49,76-78]. The dissociation constants of the competitors (*Ki*) were calculated from the corresponding IC50 values using the following equation: $Ki = [IC50]/1+[1\text{-NPN}]/K_{1\text{-NPN}}$. [IC50] was defined as the concentration of a competitor that caused a 50% reduction in the fluorescence intensity. [1-NPN] represented the free concentration of 1-NPN, and $K_{1\text{-NPN}}$ represented the dissociation constant of the complex protein/1-NPN [76].

10 Colocalization of transmission electron microscopy (TEM) and immunocytochemistry

The antennae lemalla of adult beetles were excised and chemically fixed in a mixture of paraformaldehyde (4%) and glutaraldehyde (2%) in 0.1 M phosphate-buffered saline (pH 7.4). After dehydration in an ethanol series, the samples were embedded in LR White resin (Taab, Aldermaston, Berks, UK). Ultrathin sections were cut using a diamond knife and initially treated with primary antisera against HoblOBPs, which were diluted at 1:3000–1:10000. The secondary antibody was anti-mouse IgG conjugated to 5-nm colloidal gold or anti-rabbit IgG conjugated to 10-nm colloidal gold (Sigma, St. Louis, MO), which was diluted to a ratio of 1:20. Gold granules were amplified using silver-intensification. Next, the sections were stained with 2% uranyl acetate to increase the contrast for transmission electron microscopy analysis (HITACHIH-7500) [63,68,79,80].

Double-labelling for HoblOBP1 and HoblOBP2 or HoblOBP2 and HoblOBP4 was performed using both antisera on the same grid, according to a previously described method [80]. For HoblOBP2 and HoblOBP4 double-labelling, the primary HoblOBP2 antibodies were incubated for 120 min at room temperature and subsequently incubated with goat-anti-rabbit IgG conjugated with 10-nm gold, as described above. Silver enhancement was then performed. Next, the sections were labeled using HoblOBP4 antibodies and goat-anti-mouse IgG conjugated with 5-nm gold without silver enhancement. Then, 2% uranyl acetate was used to stain the sections. The two labels could be easily discriminated from each other. This double-labelling method for HoblOBP1 and HoblOBP2 was performed with silver enhancement again after the second labeling.

Acknowledgements

We are grateful to HongJing Hao and Ying Wang for skillful technical assistance in transmission electron microscopy, as well as Sisi Deng and Xujing Zhuang for valuable proposals. We also want to thank anonymous editors of Elsevier Language Editing Services for providing language editing help.

Author Contributions

Conceived and designed the experiments: JY BW YZC. Performed the experiments: BW LG. Analyzed the data: BW JY. Contributed reagents/materials/analysis tools: JY BW YZC KBL TZ. Wrote the manuscript: BW.

References

1. Field LM, Pickett JA, Wadhams LJ (2000) Molecular studies in insect olfaction. Insect Mol Biol 9: 545–551. doi:10.1046/j.1365-2583.2000.00221.x. PubMed: 11122463.
2. Zubkov S, Gronenborn AM, Byeon IL, Mohanty S (2005) Structural consequences of the pH-induced conformational switch in *A. polyphemus* pheromone-binding protein: mechanisms of ligand Release. J Mol Biol 354: 1081–1090. doi:10.1016/j.jmb.2005.10.015. PubMed: 16289114.
3. Jiang QY, Wang WX, Zhang ZD, Zhang L (2009) Binding specificity of locust odorant binding protein and its key binding site for initial recognition of alcohols. Insect Biochem Mol Biol 39: 440–447. doi:10.1016/j.ibmb.2009.04.004. PubMed: 19376226.
4. Biessmann H, Andronopoulou E, Biessmann MR, Douris V, Dimitratos SD et al. (2010) The *Anopheles gambiae* odorant binding protein 1 (AgamOBP1) mediates indole recognition in the antennae of female

mosquitoes. PLOS ONE 5(3): e9471. doi:10.1371/journal.pone.0009471. PubMed: 20208991.
5. Zhong T, Yin J, Deng SS, Li KB, Cao YZ (2012) Fluorescence competition assay for the assessment of green leaf volatiles and trans-β-farnesene bound to three odorant-binding proteins in the wheat aphid *Sitobion avenae* (Fabricius). J Insect Physiol 58: 771–778. doi:10.1016/j.jinsphys.2012.01.011. PubMed: 22306433.
6. Leal WS (2013) Odorant reception in insects: roles of receptors, binding proteins, and degrading enzymes. Annu Rev Entomol 58: 373–391. doi:10.1146/annurev-ento-120811-153635. PubMed: 23020622.
7. Pelosi P, Zhou JJ, Ban LP, Calvello M (2006) Soluble proteins in insect chemical communication. Cell Mol Life Sci 63: 1658–1676. doi:10.1007/s00018-005-5607-0. PubMed: 16786224.
8. Zhou JJ, Robertson G, He X, Dufour S, Hooper AM et al. (2009) Characterisation of *Bombyx mori* Odorant-binding proteins reveals that a general odorant-binding protein discriminates between sex pheromone components. J Mol Biol 389: 529–545. doi:10.1016/j.jmb.2009.04.015. PubMed: 19371749.
9. Leal WS, Nikonova L, Peng G (1999) Disulfide structure of the pheromone binding protein from the silkworm moth, *Bombyx mori*. FEBS Lett 464: 85–90. doi:10.1016/S0014-5793(99)01683-X. PubMed: 10611489.
10. Scaloni A, Monti M, Angeli S, Pelosi P (1999) Structural analyses and disulfide-bridge pairing of two odorant binding proteins from *Bombyx mori*. Biochem Biophys Res Commun 266: 386–391. doi:10.1006/bbrc.1999.1791. PubMed: 10600513.
11. Briand L, Nespoulous C, Huet J C, Takahashi M, Pernollet JC (2001) Ligand binding and physico-chemical properties of ASP2, a recombinant odorant-binding protein from honeybee (*Apis mellifera* L.). European Journal of Biochemistry 268: 752–760
12. Calvello M, Guerra N, Brandazza A, Ambrosio CD, Scaloni A et al. (2003) Soluble proteins of chemical communication in the social wasp *Polistes dominulus*. Cellular and Molecular Life Sciences 60: 1933–1943. doi:10.1007/s00018-003-3186-5. PubMed: 14523553.
13. Deng SS, Yin J, Zhong T, Cao YZ, Li KB (2012) Function and immunocytochemical localisation of two novel odorant-binding proteins in olfactory sensilla of the scarab beetle *Holotrichia oblita* Fald (Coleoptera: Scarabaeidae). Chem Senses 37: 141–150. doi:10.1093/chemse/bjr084. PubMed: 21852709.
14. Yin J, Feng HL, Sun HY, Xi JH, Cao YZ, et al. (2012) Functional analysis of general odorant binding protein 2 from the Meadow Moth, *Loxostege sticticalis* L. (Lepidoptera: Pyralidae). PLoS ONE 7(3): e33589
15. Vogt RG, Riddiford LM (1981) Pheromone binding and inactivation by moth antennae. Nature 293: 161–163. doi:10.1038/293161a0. PubMed: 18074618.
16. McKenna MP, Hekmat-Scafe DS, Gaines P, Carlson JR (1994) Putative Drosophila pheromone-binding proteins expressed in a subregion of the olfactory system. J Biol Chem 269: 16340–16347. PubMed: 8206941.
17. Pikielny CW, Hasan G, Rouyer F, Rosbash M (1994) Members of a family of *Drosophila* putative odorant-binding proteins are expressed in different subsets of olfactory hairs. Neuron 12: 35–49. doi:10.1016/0896-6273(94)90150-3. PubMed: 7545907.
18. Maleszka R, Stange G (1997) Molecular cloning, by a novel approach, of a cDNA encoding a putative olfactory protein in the labial palps of the moth *Cactoblastis cactorum*. Gene 202: 39–43. doi:10.1016/S0378-1119(97)00448-4. PubMed: 9427543.
19. Angeli S, Ceron F, Scaloni A, Monti M, Monteforti G et al. (1999) Purification, structural characterization, cloning and immunocytochemical localization of chemoreception proteins from *Schistocerca gregaria*. Eur J Biochem 262: 745–754. doi:10.1046/j.1432-1327.1999.00438.x. PubMed: 10411636.
20. Jin X, Brandazza A, Navarrini A, Ban L, Zhang S et al. (2005) Expression and immunolocalisation of odorant-binding and chemosensory proteins in locusts. Cell Mol Life Sci 62: 1156–1166. doi:10.1007/s00018-005-5014-6. PubMed: 15928808.
21. González D, Zhao Q, McMahan C, Velasquez D, Haskins WE et al. (2009) The major antennal chemosensory protein of red imported fire ant workers. Insect Mol Biol 18: 395–404. doi:10.1111/j.1365-2583.2009.00883.x. PubMed: 19523071.
22. Gu SH, Wang SY, Zhang XY, Ji P, Liu JT et al. (2012) Functional characterizations of chemosensory proteins of the alfalfa plant bug *Adelphocoris lineolatus* indicate their involvement in host recognition. PLOS ONE 7(8): e42871. doi:10.1371/journal.pone.0042871. PubMed: 22900060.
23. Liu R, He X, Lehane S, Lehane M, Hertz-Fowler C et al. (2012) Expression of chemosensory proteins in the tsetse fly *Glossina morsitans* is related to female host-seeking behavior. Insect Mol Biol 21: 41–48. doi:10.1111/j.1365-2583.2011.01114.x. PubMed: 22074189.
24. Nomura A, Kawasaki K, Kubo T, Natori S (1992) Purification and localization of p10, a novel protein that increases in nymphal regenerating legs of *Periplaneta americana* (American cockroach). Int J Dev Biol 36: 391–398. PubMed: 1445782.
25. Kitabayashi AN, Arai T, Kubo T, Natori S (1998) Molecular cloning of cDNA for p10, a novel protein that increases in the regenerating legs of *Periplaneta americana* (American cockroach). Insect Biochem Mol Biol 28: 785–790. doi:10.1016/S0965-1748(98)00058-7. PubMed: 9807224.
26. Ban LP, Scaloni A, Brandazza A, Angeli S, Zhang L et al. (2003) Chemosensory proteins of *Locusta migratoria*. Insect Mol Biol 12: 125–134. doi:10.1046/j.1365-2583.2003.00394.x. PubMed: 12653934.
27. Zhou SH, Zhang J, Zhang SG, Zhang L (2008) Expression of chemosensory proteins in hairs on wings of *Locusta migratoria* (Orthoptera: Acrididae). Journal of Applied Entomology 132: 439–450. doi:10.1111/j.1439-0418.2007.01255.x.
28. Kaissling KE (1998) A quantitative model of odor deactivation based on the redox shift of the pheromone-binding protein in moth antennae. Ann N Y Acad Sci 855: 320–322. doi:10.1111/j.1749-6632.1998.tb10590.x. PubMed: 10049225.
29. Kaissling KE (2001) Olfactory perireceptor and receptor events in moths: a kinetic model. Chem Senses 26: 125–150. doi:10.1093/chemse/26.2.125. PubMed: 11238244.
30. Kaissling KE (2004) Physiology of pheromone reception in insects. ANIR 6: 73–91.
31. Lee D, Damberger FF, Peng G, Horst R, Güntert P et al. (2002) NMR structure of the unliganded *Bombyx mori* pheromone-binding protein at physiological pH. FEBS Lett 531: 314–318. doi:10.1016/S0014-5793(02)03548-2. PubMed: 12417333.
32. Klusák V, Havlas Z, Rulísek L, Vondrásek J, Svatos A (2003) Sexual attraction in the silkworm moth. Nature of binding of bombykol in pheromone binding protein-an ab initio study. Chem Biol 10: 331–340. doi:10.1016/S1074-5521(03)00074-7. PubMed: 12725861.
33. Lartigue A, Gruez A, Spinelli S, Rivière S, Brossut R et al. (2003) The crystal structure of a cockroach pheromone-binding protein suggests a new ligand binding and release mechanism. J Biol Chem 278: 30213–30218. doi:10.1074/jbc.M304688200. PubMed: 12766173.
34. Mohanty S, Zubkov S, Gronenborn AM (2004) The solution NMR structure of *Antheraea polyphemus* PBP provides new insight into pheromone recognition by pheromone-binding proteins. J Mol Biol 337: 443–451. doi:10.1016/j.jmb.2004.01.009. PubMed: 15003458.
35. Xu X, Xu W, Rayo J, Ishida Y, Leal WS et al. (2010) NMR structure of navel orangeworm moth pheromone-binding protein (AtraPBP1): implications for pH-sensitive pheromone detection. Biochemistry 49: 1469–1476. doi:10.1021/bi9020132. PubMed: 20088570.
36. Xu W, Xu X, Leal WS, Ames JB (2011) Extrusion of the C-terminal helix in navel orangeworm moth pheromone-binding protein (AtraPBP1) controls pheromone binding. Biochem Biophys Res Commun 404: 335–338. doi:10.1016/j.bbrc.2010.11.119. PubMed: 21130734.
37. Wogulis M, Morgan T, Ishida Y, Leal WS, Wilson DK (2006) The crystal structure of an odorant binding protein from *Anopheles gambiae*: evidence for a common ligand release mechanism. Biochem Biophys Res Commun 339: 157–164. doi:10.1016/j.bbrc.2005.10.191. PubMed: 16300742.
38. Leite NR, Krogh R, Xu W, Ishida Y, Iulek J et al. (2009) Structure of an odorant-binding protein from the mosquito *Aedes aegypti* suggests a binding pocket covered by a pH-sensitive "Lid". PLOS ONE 4: e8006. doi:10.1371/journal.pone.0008006. PubMed: 19956631.
39. Mao Y, Xu X, Xu W, Ishida Y, Leal WS et al. (2010) Crystal and solution structures of an odorant-binding protein from the southern house mosquito complexed with an oviposition pheromone. Proc Natl Acad Sci U S A 107: 19102–19107. doi:10.1073/pnas.1012274107. PubMed: 20956299.
40. Laughlin JD, Ha TS, Jones DNM, Smith DP □2008,) Activation of pheromone-sensitive neurons is mediated by conformational activation of pheromone-binding protein. Cell 133: 1255–1265. doi:10.1016/j.cell.2008.04.046. PubMed: 18585358.
41. Pophof B (2002) Moth pheromone binding proteins contribute to the excitation of olfactory receptor cells. Naturwissenschaften 89: 515–518. doi:10.1007/s00114-002-0364-5. PubMed: 12451455.
42. Xu P, Atkinson R, Jones DN, Smith DP (2005) *Drosophila* OBP LUSH is required for activity of pheromone-sensitive neurons. Neuron 45: 193–200. doi:10.1016/j.neuron.2004.12.031. PubMed: 15664171.
43. Andronopoulou E, Labropoulou V, Douris V, Woods DF, Biessmann H, Iatrou K (2006) Specific interactions among odorant-binding proteins of the African malaria vector *Anopheles gambiae*. Insect Mol Biol 15: 797–811. doi:10.1111/j.1365-2583.2006.00685.x. PubMed: 17201772.

44. Qiao HL, He XL, Schymura D, Ban LP, Field L et al. (2011) Cooperative interactions between odorant-binding proteins of *Anopheles gambiae*. Cellular and Molecular Life Sciences 68: 1799–1813. doi:10.1007/s00018-010-0539-8. PubMed: 20957509.
45. Campanacci V, Longhi S, Nagnan-Le Meillour P, Cambillau C, Tegoni M (1999) Recombinant pheromone binding protein 1 from *Mamestra brassicae* (MbraPBP1). European Journal of Biochemistry 264: 707–716. doi:10.1046/j.1432-1327.1999.00666.x. PubMed: 10491116.
46. Danty E, Briand L, Michard-Vanhée C, Perez V, Arnold G et al. (1999) Cloning and expression of a queen pheromone-binding protein in the honeybee: an olfactory-specific, developmentally regulated protein. Journal of Neuroscience 19: 7468–7475. PubMed: 10460253.
47. Plettner E, Lazar J, Prestwich EG, Prestwich GD (2000) Discrimination of pheromone enantiomers by two pheromone binding proteins from the gypsy moth *Lymantria dispar*. Biochemistry 39: 8953–8962. doi: 10.1021/bi000461x. PubMed: 10913308.
48. Sandler BH, Nikonova L, Leal WS, Clardy J (2000) Sexual attraction in the silkworm moth: structure of the pheromone-binding protein-bombykol complex. Chem Biol 7: 143–151. doi:10.1016/S1074-5521(00)00078-8. PubMed: 10662696.
49. Ban LP, Scaloni A, D'Ambrosio C, Zhang L, Yahn YH et al. (2003) Biochemical characterization and bacterial expression of an odorant-binding protein from *Locusta migratoria*. Cellular and Molecular Life Sciences 60: 390–400. doi:10.1007/s000180300032. PubMed: 12678502.
50. Leal WS, Sawada M, Matsuyama S, Kuwahara Y, Hasegawa M (1993) Unusual periodicity of sex pheromone production in the large black chafer *Holotrichia parallela*. J Chem Ecol 19(7): 1381–1391. doi: 10.1007/BF00984883. PubMed: 24249169.
51. Hu JH, Wang ZY, Sun F (2011) Anatomical organization of antennal-lobe glomeruli in males and females of the scarab beetle *Holotrichia diomphalia* (Coleoptera: Melolonthidae). Arthropod Struct Dev 40: 420–428. doi:10.1016/j.asd.2011.03.003. PubMed: 21889404.
52. Ju Q, Qu MJ, Wang Y, Jiang XJ, Li X et al. (2012) Molecular and biochemical characterization of two odorant-binding proteins from dark black chafer, *Holotrichia parallela*. Genome 55: 537–546. doi:10.1139/g2012-042. PubMed: 22799437.
53. Mueller D, Pierce L, Benezet H, Krischik V (1990) Practical application of pheromone traps in food and tobacco industry. Journal of the Kansas Entomological Society 63(4): 548–553.
54. Leal WS (1998) Chemical ecology of phytophagous scarab beetles. Annu Rev Entomol 43(1): 39–61. doi:10.1146/annurev.ento.43.1.39. PubMed: 15012384.
55. The Tribolium Genome Sequencing Consortium (2008) The genome of the model beetle and pest *Tribolium castaneum*. Nature 452: 949–955. doi:10.1038/nature06784. PubMed: 18362917.
56. Prestwich GD (1993) Bacterial expression and photoaffinity labeling of a pheromone binding protein. Protein Sci 2: 420–428. PubMed: 8453379.
57. Ziemba BP, Murphy EJ, Edlin HT, Jones DN (2013) A novel mechanism of ligand binding and release in the odorant binding protein 20 from the malaria mosquito *Anopheles gambiae*. Protein Sci 22(1): 11–21. doi:10.1002/pro.2179. PubMed: 23081820.
58. Schwede T, Kopp J, Guex N, Peitsch MC (2003) SWISS-MODEL: an automated protein homology-modeling server. Nucleic Acids Res 31: 3381–3385. doi:10.1093/nar/gkg520. PubMed: 12824332.
59. Leal WS, Matsuyama S, Kuwahara Y, Wakamura S, Hasegawa M (1992) An amino acid derivative as the sex pheromone of a scarab beetle. Naturwissenschafte 79: 184–185. doi:10.1007/BF01134440.
60. Wang H (2002) A preliminary study on sex pheromone component *Holotrichia oblita* Faldermann. Journal of Northwest Sci-Tech University of Agriculture and Forestry 30: 91–95
61. Deng SS, Yin J, Cao YZ, Luo ZX, Wang W et al. (2011) Electroantennographic and behavioral responses of *Holotrichia oblita* (Faldermann) (Coleoptera:Scarabaeidae) to plant volatiles. Plant Protection 37(5): 62–66.
62. Lartigue A, Gruez A, Briand L, Blon F, Bézirard V et al. (2004) Sulfur single-wavelength anomalous diffraction crystal structure of a pheromone-binding protein from the honeybee *Apis mellifera* L. J Biol Chem 279: 4459–4464. PubMed: 14594955.
63. Steinbrecht RA, Laue M, Ziegelberger G (1995) Immunolocalization of pheromone-binding protein and general odorant-binding protein in olfactory sensilla of the silk moths *Antheraea* and *Bombyx*. Cell and Tissue Research 282: 203-217. doi:10.1007/BF00319112.
64. Steinbrecht RA, Ozaki M, Ziegelberger G (1992) Immunocytochemical localization of pheromone-binding protein in moth antennae. Cell and Tissue Research 270: 287–302. doi:10.1007/BF00328015.
65. Laue M, Steinbrecht RA, Ziegelberger G (1994) Immunocytochemical localization of general odorant-binding protein in olfactory sensilla of the silkmoth *Antheraea polyphemus*. Naturwissenschaften 81: 178–180. doi:10.1007/s001140050052.
66. Zhang SG, Maida R, Steinbrecht A (2001) Immunolocalization of odorant-binding proteins in noctuid moths (Insecta, Lepidoptera). Chem Senses 26: 885–896. doi:10.1093/chemse/26.7.885. PubMed: 11555483.
67. Hekmat-Scafe DS, Steinbrecht RA, Carlson JR (1997) Coexpression of two odorant-binding protein homologs in *Drosophila*: implications for olfactory coding. J Neurosci 17: 1616–1624. PubMed: 9030621.
68. Shanbhag SR, Smith DP, Steinbrecht RA (2005) Three odorant-binding proteins are co-expressed in sensilla trichodea of *Drosophila melanogaster*. Arthropod Structure and Development 34: 153–165. doi: 10.1016/j.asd.2005.01.003.
69. Hekmat-Scafe DS, Scafe CR, McKinney AJ, Tanouye MA (2002) Genome-wide analysis of the odorant-binding protein gene family in *Drosophila melanogaster*. Genome Res 12: 1357–1369. doi: 10.1101/gr.239402. PubMed: 12213773.
70. Bendtsen JD, Nielsen H, Heijne GV, Brunak S (2004) Improved prediction of signal peptides: SignalP 3.0. Journal of Molecular Biology 340: 783–795
71. Thompson JD, Gibson TJ, Plewniak F, Jeanmougin F, Higgins DG (1997) The Clustal_X windows interface: flexible strategies for multiple sequence alignment aided by quality analysis tools. Nucleic Acids Res 25: 4876–4882. doi:10.1093/nar/25.24.4876. PubMed: 9396791.
72. Tamura K (2007) MEGA4: Molecular Evolutionary Genetics Analysis (MEGA) software version 4.0. Mol Biol Evol 24: 1596–1599. doi: 10.1093/molbev/msm092. PubMed: 17488738.
73. Sun YF, De Biasio F, Qiao HL, Iovinella I, Yang SX et al. (2012) Two odorant-binding proteins mediate the behavioural response of aphids to the alarm pheromone (E)-β-Farnesene and structural analogues. PLOS ONE 7(3): e32759. doi:10.1371/journal.pone.0032759. PubMed: 22427877.
74. Ramachandran GN, Ramakrishnan C, Sasisekharan V (1963) Stereochemistry of polypeptide chain configurations. J Mol Biol 7: 95–99. doi:10.1016/S0022-2836(63)80023-6. PubMed: 13990617.
75. Bradford MM (1976) A rapid and sensitive for the quantitation of microgram quantitites of protein utilizing the principle of protein-dye binding. Anal Biochem 72: 248–254. doi: 10.1016/0003-2697(76)90527-3. PubMed: 942051.
76. Campanacci V, Krieger J, Bette S, Sturgis JN, Lartigue A et al. (2001) Revisiting the specificity of *Mamestra brassicae* and *Antheraea polyphemus* pheromone-binding proteins with a fluorescence binding assay. J Biol Chem 276: 20078–20084. doi:10.1074/jbc.M100713200. PubMed: 11274212.
77. Ban LP, Zhang L, Yan YH, Pelosi P (2002) Binding properties of a locust's chemosensory protein. Biochem Biophys Res Commun 293: 50–54. doi:10.1016/S0006-291X(02)00185-7. PubMed: 12054562.
78. Dani FR, Iovinella I, Felicioli A, Niccolini A, Calvello MA et al. (2010) Mapping the expression of soluble olfactory proteins in the honeybee. J Proteome Res 9: 1822–1833. doi:10.1021/pr900969k. PubMed: 20155982.
79. Danscher G (1981) Localization of gold in biological tissue: a photochemical method for light and electronmicroscopy. Histochemistry 71: 81–88. doi:10.1007/BF00592572. PubMed: 6785260.
80. Bienz K, Egger D, Pasamontes L (1986) Electron microscopic immunocytochemistry. Silver enhancement of colloidal gold marker allows double labeling with the same primary antibody. J Histochem Cytochem 34: 1337–1342. doi:10.1177/34.10.3745912. PubMed: 3745912.